

**Neuron, Volume 69**

**Supplemental Information**

## **The Dendritic Branch Is the Preferred Integrative Unit for Protein Synthesis-Dependent LTP**

**Arvind Govindarajan, Inbal Israely, Shu-Ying Huang, and Susumu Tonegawa**

### **Supplemental Experimental Procedures**

**Organotypic mouse hippocampal slice cultures, reagents and solutions.** Hippocampal slice cultures were prepared from postnatal day 7-10 mice as described (Stoppini et al., 1991). Briefly, 350  $\mu\text{m}$  thick slices were made with a chopper in ice-cold ACSF (see below) containing 1mM  $\text{MgCl}_2$ , 5mM  $\text{CaCl}_2$ , and 24mM sucrose, and cultured on membranes (Millipore). The slices were fed with media in an interface configuration using 1x MEM (Invitrogen) supplemented with 20% horse serum (Invitrogen), L-glutamine, 27mM D-glucose, 6mM  $\text{NaHCO}_3$ , 2mM  $\text{CaCl}_2$ , 2mM  $\text{MgSO}_4$ , 30mM HEPES, 1.2% ascorbic acid, 1 $\mu\text{g}/\text{mL}$  insulin, and pH adjusted to 7.3, and osmolarity adjusted to 300-310 mOsm. Mice were sacrificed according to MIT Committee for Animal Care guidelines. Slices were transfected by biolistic gene transfer with gold beads (10 mg, 1.6  $\mu\text{m}$  diameter, Biorad) coated with Dendra (Evrogen) plasmid DNA (100 $\mu\text{g}$ ) using a Biorad Helios gene gun after 7–10 days *in vitro* (DIV). Experiments were performed 2–5 days post-transfection, at room temperature.

MNI-L-glutamate (2.5 mM), forskolin (50  $\mu\text{M}$ ), SKF38393 (100 $\mu\text{M}$ ) cycloheximide (60 $\mu\text{M}$ ) and anisomycin (50  $\mu\text{M}$ ) were from Tocris. PicROTOXIN (PcTx, 50  $\mu\text{M}$ ), amphotericin B (0.5mg/mL) and TTX (tetrodotoxin, 0.5 $\mu\text{M}$ ) were from Sigma. Alexa 594 dye (30mM) was from Invitrogen.

During the experiments, slices were perfused with carbogenated (95% O<sub>2</sub>, 5% CO<sub>2</sub>) artificial cerebral spinal fluid (ACSF) containing the following (in mM): 127 NaCl, 25 NaHCO<sub>3</sub>, 25 D-glucose, 2.5 KCl, 1 MgCl<sub>2</sub>, 2 CaCl<sub>2</sub> and 1.25 NaH<sub>2</sub>PO<sub>4</sub> and TTX, delivered with a peristaltic pump at 1.5 ml / min. Uncaging ACSF (uACSF) was the same as ACSF except for 4 mM CaCl<sub>2</sub>, 0 mM MgCl<sub>2</sub>, PcTx, MNI-glutamate, 0 TTX, forskolin (L-LTP only), anisomycin (depending on the experiment). DMSO was added to the ACSF to control for the trace amounts (<0.25%) used to deliver PcTx, forskolin, anisomycin and cycloheximide in the uACSF and during the anisomycin incubations. For the experiments in Fig. S1D-E, S2A, the uACSF differed in that it contained 2mM CaCl<sub>2</sub> and no picrotoxin, while the ACSF contained no TTX. For the pseudosynchronous stimulation experiments, the ACSF contained no TTX, and the uACSF was the same as the ACSF except for the addition of SKF38393 (for L-LTP induction only). Cycloheximide was substituted for anisomycin in some experiments and SKF38393 was substituted for forskolin in some experiments (noted in the text).

**Acute mouse hippocampal slices.** Hippocampal slices were prepared from 7-9 week old Thy1-GFP GFP-M line (Feng et al., 2000). Briefly, 300 μm thick slices were made with a chopper in ice-cold ACSF containing 1mM MgCl<sub>2</sub>, 2mM CaCl<sub>2</sub>, and incubated for 3hrs in a humidified carbogenated chamber on a filter-paper (Whatman) interface soaked with ACSF at room temperature. Slices were incubated in the microscope for an additional 1hr. while being perfused with 32°C ACSF, and all experiments were done at 32°C.

**Imaging.** Two-photon imaging and glutamate uncaging were performed using a modified Olympus FV 1000 multiphoton with SIM scanner on a BX61WI microscope with two Ti:sapphire lasers (910nm for imaging Dendra and 720nm for uncaging; MaiTai, Spectra Physics) controlled by Olympus Fluoview software. The system contains acousto-optical modulators to control the intensity of each beam. The objective used was a LUMPlanFI/IR 60x 0.9 NA (Olympus). Two sets of steering mirrors were used to align the beams: first coarsely at

the center of the back focal plane of the objective, and then a second fine alignment was carried out by imaging 0.5  $\mu\text{m}$  fluorescent beads at the sample plane, imaged simultaneously with both beams until the images overlapped. The precise three-dimensional beam alignment was confirmed at the start of each experimental day, both by ensuring that the images of the beads were perfectly aligned in all three axes, and via bleaching of a single bead targeted based on the 910nm image, but bleached with the 720nm laser. Imaging was started 45min – 1 hour after slice incubation began.

**Glutamate Uncaging.** MNI-caged-L-glutamate was dissolved in ACSF (without TTX, PcTX,  $\text{MgCl}_2$  or  $\text{CaCl}_2$ ) in the dark at a stock concentration of 10 mM, and individual aliquots were diluted to the working concentration of 2.5 mM in uACSF in 3 ml volumes. Large stocks of MNI-glutamate were prepared and aliquoted, and each batch of stock MNI-glutamate was tested using whole-cell patch clamp electrophysiology and single spine uncaging (see below for method) to ensure no measurable levels of glutamate prior to uncaging (measured by changes in membrane potential), and to ensure that uEPSCs had the same amplitude and waveform as mEPSCs. Spines for all electrophysiology experiments, as well as Figures 4, 6, 7 were chosen from the most proximal tertiary apical branches, counting the apical trunk as the primary branch. Stimulation was performed by substituting uACSF for ACSF in a closed circulation system with continued carbogenation, and 5 minutes later, uncaging was started, using the 720 nm laser beam which was manually positioned approximately 0.5 $\mu\text{m}$  from the tip of the spine head away from the parent dendrite. During the stimulus trains for the single spine stimulation protocol, we used pulses lasting 4 ms for the LTP protocols at 0.5 Hz for 1 minute (30 pulses) and lasting 1 ms for the subthreshold protocol as previously described (Harvey and Svoboda, 2007). A 0.1ms pulse with 10mM MNI-Glutamate concentration in the uACSF was used for the experiments in Fig. S5A-C (Losonczy and Magee, 2006; Losonczy et al., 2008). It is to be noted that the only difference between L-LTP and E-LTP was the presence or absence of forskolin in the uACSF. For test pulses and for electrophysiological experiments, the uACSF was the same as the ACSF

except for the presence of the MNI-Glutamate. The uACSF was present in those cases throughout the experiment, and the pulses were 1ms long. The intensity of the laser light used depended on the batch as described below. Immediately after the termination of the uncaging pulses, ACSF was reintroduced to substitute the uACSF. In some cases, as described in the text, the D1R agonist SKF38393 was used in place of forskolin. For pseudosynchronous stimulation, Dendra-expressing cells were scanned till one was found with the most proximal apical tertiary dendrite containing enough spines on the same z-plane as needed for the experiment. In addition, it was verified (using the Fluoview software) that the spines could be stimulated within 6ms. These spines were stimulated with 0.1ms pulses starting at one end and proceeding to the other end in a linear fashion. For the single branch cases, approximately 50% of experiments had the spines stimulated with the proximal spines first and proceeding to the distal and vice versa. For the sister branch cases, spines at the distal end of either branch was stimulated first, proceeding towards the branch point and then proceeding towards the distal end of the neighboring branch. Different orders of stimulation were not possible because it would severely increase the time between the first spine stimulation and the last.

**Electrophysiology.** The internal solution contained (in mM): 136.5 potassium gluconate, 17.5 KCl, 9 NaCl, 1 MgCl<sub>2</sub>, 10 HEPES, 0.2 EGTA, and 0.03 Alexa 594. For perforated-patch experiments (Fig. 1B-C) used 0.5 mg/ml amphotericin B in the internal solution. Perforations reached a stable series resistance ( $28 \pm 10 \text{ M}\Omega$ ) within 30–45 min of seal formation. Whole-cell breakin was detected as a dialysis of the Dendra in the cell concomitant with Alexa 594 entering the cell. Series resistances were checked for stability during the experiment ( $\pm 20\%$ ). uEPSCs were measured in response to test stimuli (1ms. every 10 min) at -70 mV. uEPSC amplitudes were measured as the difference between the mean current amplitude over a 5-ms window around the peak and the mean current amplitude over a 100-ms window before the uncaging stimulus. Each time point is the average of five trials at 0.1Hz (Reanalysis of the data using the maximum of the five trials is shown in the supplementary figures). Recordings were done with

an Axopatch 200B amplifier, filtered at 2kHz, data digitized with a Digidata 1440 at 10kHz, and recorded using pClamp 10 (Axon). Recordings were synchronized with uncaging via a TTL pulse sent by Fluoview to the Digidata 1440. For whole-cell recordings (Fig. S1F, Fig. S3, Table 1, MNI-Glutamate batch testing), the series resistance was 13-20M $\Omega$ , and the cells visualized using Alexa 488 present in the patch pipette.

To standardize each batch of MNI-Glutamate, 1ms test pulses were given to multiple spines across (avg. 5 spines / dendritic branch, 3 cells) to determine the intensity of laser light that resulted in uEPSCs with the same amplitude as a mEPSC. In general, this was found to be ~60mW delivered to the back focal aperture. For the stimulus trains, we used ~30mW pulses lasting 4ms. Similar calibration was done for 0.1ms pulses. In Fig. S3H, where uEPSCs are compared to mEPSCs, mEPSCs were measured in ACSF containing TTX and picrotoxin to eliminate evoked EPSCs and IPSCs, respectively. mEPSCs were detected using a template search in Clampfit 10 (Axon). For Fig. S1F, recordings were done in current-clamp mode. Anisomycin, and cycloheximide, when present, were introduced to the slice 15min prior to stimulation. They were not present on the slices for more than 75 min, due to reduction in Dendra fluorescence.

**Data analysis and Statistics.** Spine volumes were measured as previously described (Tanaka et al., 2008). Briefly, individual 3D ROIs containing the spine of interest were registered using TurboReg (Thevenaz et al., 1998) (Biomedical Imaging Group, EPFL), and Z-stacked. The full width at half maximum (FWHM) of the spine head was then measured, and the volume of the spine calculated based on the volume of a sphere using the diameter as the FWHM of the spine head. The measures were performed in ImageJ (NIH) with a custom written plugin that performed image registration, and a best fit analysis of the FWHM for each time point. An alternate method exists for estimating spine volume from the ratio of integrated fluorescence intensity of the spine to the integrated fluorescence intensity of the parent dendrite (Harvey and

Svoboda, 2007). Since we were studying protein synthesis-dependent plasticity, and several of our experiments used protein synthesis inhibitors, we decided to use the FWHM method to remove any possible confounds caused by changes in reporter levels in the spine / dendrite and LTP-induced changes in spine neck diffusion (Bloodgood and Sabatini, 2005). All normalization was performed on a per spine basis as a percent of the average baseline value for the spine.

### **Supplemental Figure Legends:**

**Supplemental Figure 1 (related to Fig. 1): Additional data supporting the demonstration of L-LTP and E-LTP at single spines.** **A)** Pooled data from 8 experiments show that GLU+FSK stimulation at a single spine resulted in robust spine growth of the stimulated spine but not neighboring spines. **B)** Data from Fig. 1B (4 experiments) plotted such that the uEPSC amplitude for each spine at each time point is the maximum of 5 measurements instead of the average as plotted in Fig. 1B. Scale bar represents 10ms and 20pA. **C)** Linear regression analysis of the data from Fig. 1B shows that there was a strong correlation between the uEPSC amplitude (taken as the average of 5 measurements) and the spine volume. **D)** This correlation was also visible when the maximum of 5 uEPSC amplitudes per time-point was used in the analysis instead of the average of 5 uEPSC amplitudes. **E)** Pooled data from 5 experiments show that GLU+FSK stimulation at a single spine resulted in robust spine growth of the stimulated spine but not neighboring spines similarly to Fig. S1A., in conditions with no TTX, picrotoxin and with 2mM  $\text{Ca}^{+2}$ . **F)** Pooled data from 5 experiments show that GLU stimulation at a single spine resulted in a declining LTP, in conditions with no TTX, picrotoxin and with 2mM  $\text{Mg}^{+2}$ . **G)** Potential change in response to uncaging pulse measured at the soma using current-clamp conditions is shown in the absence and presence of forskolin (8 slices each). Scale bar represents 50ms and

0.1mV. Blue bar indicates time of forskolin addition (for 5min), blue, red arrow (A, B, E, F) or black bar (G) indicates uncaging tetanus. GLU: tetanus of glutamate uncaging (30 pulses of 4ms each at 0.5Hz) at single spine; this is used in figures S1-S4, FSK: forskolin (bath applied). Normalization performed as percent of average baseline value for each spine. All data mean +/- SEM.

**Supplemental Figure 2 (related to Fig. 2): Additional data supporting the demonstration of**

**STC at single spines. A)** Pooled data from 6 experiments show that when GLU stimulation was given to a spine after GLU+FSK stimulation was given to a nearby spine, both spines showed robust growth, demonstrating STC. Unlike the experiments in Fig. 2, the experiments here were done with no TTX or picrotoxin during the experiments, and the calcium concentration was 2mM throughout the experiments (as opposed to 4mM during stimulation in other experiments where the  $Ca^{+2}$  concentration is not explicitly stated). **B)** Pooled data from 6 experiments demonstrating that GLU+FSK stimulation resulted in robust spine growth even when protein synthesis was blocked by the use of cycloheximide (L2), if a prior GLU+FSK stimulus had been applied to another spine (STC; L1) **C)** Pooled data from 4 experiments demonstrating that the spine growth did not occur at both L1 and L2 when protein synthesis was blocked at L1 and L2 during GLU+FSK stimulation by the use of cycloheximide. **D)** Pooled data from 5 experiments show that similar to Figure 2A-C, in acute cut slices, when one spine (L1) was stimulated with GLU+FSK stimulation, and a second nearby spine (L2) was stimulated with the same stimulus with anisomycin, both spines expressed L-LTP. **E)** Pooled data from 5 experiments show that when anisomycin was present during both stimuli, neither spine expressed L-LTP. Blue bar indicates time of forskolin addition (for 5min), blue arrow indicates time of uncaging tetanus, and green bar indicates addition of cycloheximide (B-C) or anisomycin (D-E). GLU: tetanus of

glutamate uncaging at single spine, FSK: forskolin (bath applied). Normalization performed as percent of average baseline value for each spine. All data mean  $\pm$  SEM.

**Supplemental Figure 3 (related to Table 1): Linear relationship between uEPSC amplitude**

**and spine volume used for Table 1. A)** An example dendritic branch and the linear relationship between uEPSC amplitude and spine volume. Scale bar (white) indicates 10 $\mu$ m.

Electrophysiological trace scale bar (left) represents 5ms and 10pA. **B)** Pooled data from 3 experiments (marked with black, red and blue points; black points are same as in A demonstrating that the linear uEPSC amplitude-spine volume relationship held across cells when the uEPSC amplitude of each spine is taken to be the average of 5 measurements. **C)** Data from B using only the maximum amplitudes from all 5 trials per spine instead of the average uEPSC amplitude show that the linear uEPSC amplitude-spine volume relationship is not an artifact of using only the average uEPSC amplitude in the analysis for B. **D, E)** Another example of a slice from which uEPSC amplitude was correlated with spine volume using two different cells demonstrating that calibration curves are similar across cells within a slice. **F)** Data from Table 1 plotted as a graph shows that changes in spine strength were correlated with changes in spine volume. This graph uses the average of 5 uEPSC measurements per spine for the analysis. **G)** Data from experiments that resulted in F using only the maximum uEPSC amplitude from all 5 trials per spine instead of the average uEPSC amplitude (used in Table 1 and F) show that the correlation between changes in spine volume change and spine strength are not an artifact of using the average uEPSC at a spine in the analysis. **H)** Average of 50 mEPSC traces (black) and of 35 uEPSC traces (red) show that uEPSC amplitude and timecourse resemble mEPSCs. Scale bar represents 5pA and 2ms, respectively. Red bar shows time of uncaging (1ms). Normalization performed as percent of average baseline value for each spine. All data mean  $\pm$  SEM.



**Supplemental Figure 4 (related to Fig. 5): Additional data supporting competition amongst**

**spines for L-LTP expression (Fig. 5).** **A)** Pooled data from 5 experiments show that when forskolin was bath applied in the absence of glutamate uncaging, and a second spine (E2) was given GLU stimulation 30min later, E2 expressed E-LTP and not L-LTP. **B-D)** Representative experiments, showing that when two spines were stimulated 1 minute apart, the spines underwent complementary growth and shrinkage during the first 30 minutes after stimulation. However after 35 minutes, both underwent growth. **E)** Pooled data from 8 experiments show that when a third spine (L3) received GLU+FSK stimulation with anisomycin 30min after two spines (L1, L2) were stimulated with GLU+FSK without anisomycin, all three of them grew more slowly. **F)** Using the data from S4E, L3's effect on L1 and L2 was quantified by comparing the average growth of L1 and L2 30min after L3 was stimulated with the average growth of L1 and L2 in the absence of L3 stimulation (from Fig. 4A). **G)** Quantifying the data from S4E, we demonstrate that stimulating two spines prior to a later GLU+FSK stimulation reduced the efficiency of the later stimulation (L3 after L1, L2), as compared to stimulating only one spine prior to the later stimulation (L2 after only L1 from Fig. 2A, with inter-stimulus interval of 30min). Blue bar indicates time of forskolin addition (for 5min), blue, teal and red arrows indicate time of uncaging tetanus, and green bar indicates addition of anisomycin. GLU: tetanus of glutamate uncaging at single spine, FSK: forskolin (bath applied). Normalization performed as percent of average baseline value for each spine. All data mean +/- SEM.

**Supplemental Figure 5 (related to Fig. 6, 7): Additional data supporting L-LTP induced by stimulation of multiple spines (Fig. 6, 7).** **A-C)** Pooled data from 5 experiments show that L-

LTP (**A**), E-LTP (**B**) and STC (**C**) all occur when the uncaging pulse is of shorter duration (0.1ms) with a higher concentration of MNI-Glutamate (10mM) as compared to the experiments

of Fig. 1-5, S1-3 where the pulse was 4ms and the concentration of MNI-Glutamate was 2.5mM.

**D)** Frequency histogram of all spine volume data from multispine pseudosynchronous stimulation experiments shows that GLU+SKF stimulation leads to two populations of spines. Black solid curve represents all data from the baseline (prior to stimulation) period. Black dashed curve represents a Gaussian fit to the baseline data. Red solid curve represents all data from the post-stimulation period. Red dashed data represents a bimodal Gaussian fit of the post-stimulation data. All spine data that fall under the larger mode are defined to represent the potentiated state. **E)** Pooled data from 5 experiments show that the presence of anisomycin results in no spines being potentiated as a result of GLU+SKF stimulation indicating that the LTP induced is L-LTP. **F, G)** Example of spines when 14 spines were stimulated with GLU+SKF. Note the examples of spines (thick lines) that change from potentiated state to unpotentiated state and vice versa. **H)** Example of spines when 14 spines were stimulated with GLU. Blue bar indicates periods of SKF38393 addition (for 5min), blue and red arrows indicates time of uncaging tetanus, and green bar indicates addition of anisomycin (I-J). SKF: SKF38393, GLU: (Panels A-C) tetanus of glutamate uncaging (30 pulses for 4ms each at 0.5Hz). GLU: (Panels D-H) tetanus of glutamate uncaging (100 pulses for 0.1ms each at 2Hz. Tetanus applied such that for each “pulse” of the tetanus, all spines were stimulated in < 6ms). Normalization performed as percent of average baseline value for each spine. All data mean +/- SEM.

### References

- Bloodgood, B.L., and Sabatini, B.L. (2005). Neuronal activity regulates diffusion across the neck of dendritic spines. *Science* 310, 866-869.
- Feng, G., Mellor, R.H., Bernstein, M., Keller-Peck, C., Nguyen, Q.T., Wallace, M., Nerbonne, J.M., Lichtman, J.W., and Sanes, J.R. (2000). Imaging neuronal subsets in transgenic mice expressing multiple spectral variants of GFP. *Neuron* 28, 41-51.

Harvey, C.D., and Svoboda, K. (2007). Locally dynamic synaptic learning rules in pyramidal neuron dendrites. *Nature* 450, 1195-1200.

Losonczy, A., and Magee, J.C. (2006). Integrative Properties of Radial Oblique Dendrites in Hippocampal CA1 Pyramidal Neurons. *Neuron* 50, 291-307.

Losonczy, A., Makara, J.K., and Magee, J.C. (2008). Compartmentalized dendritic plasticity and input feature storage in neurons. *Nature* 452, 436-441.

Stoppini, L., Buchs, P.A., and Muller, D. (1991). A simple method for organotypic cultures of nervous tissue. *J Neurosci Methods* 37, 173-182.

Tanaka, J., Horiike, Y., Matsuzaki, M., Miyazaki, T., Ellis-Davies, G.C., and Kasai, H. (2008). Protein synthesis and neurotrophin-dependent structural plasticity of single dendritic spines. *Science* 319, 1683-1687.

Thevenaz, P., Ruttimann, U.E., and Unser, M. (1998). A pyramid approach to subpixel registration based on intensity. *IEEE Trans Image Process* 7, 27-41.

Figure S1

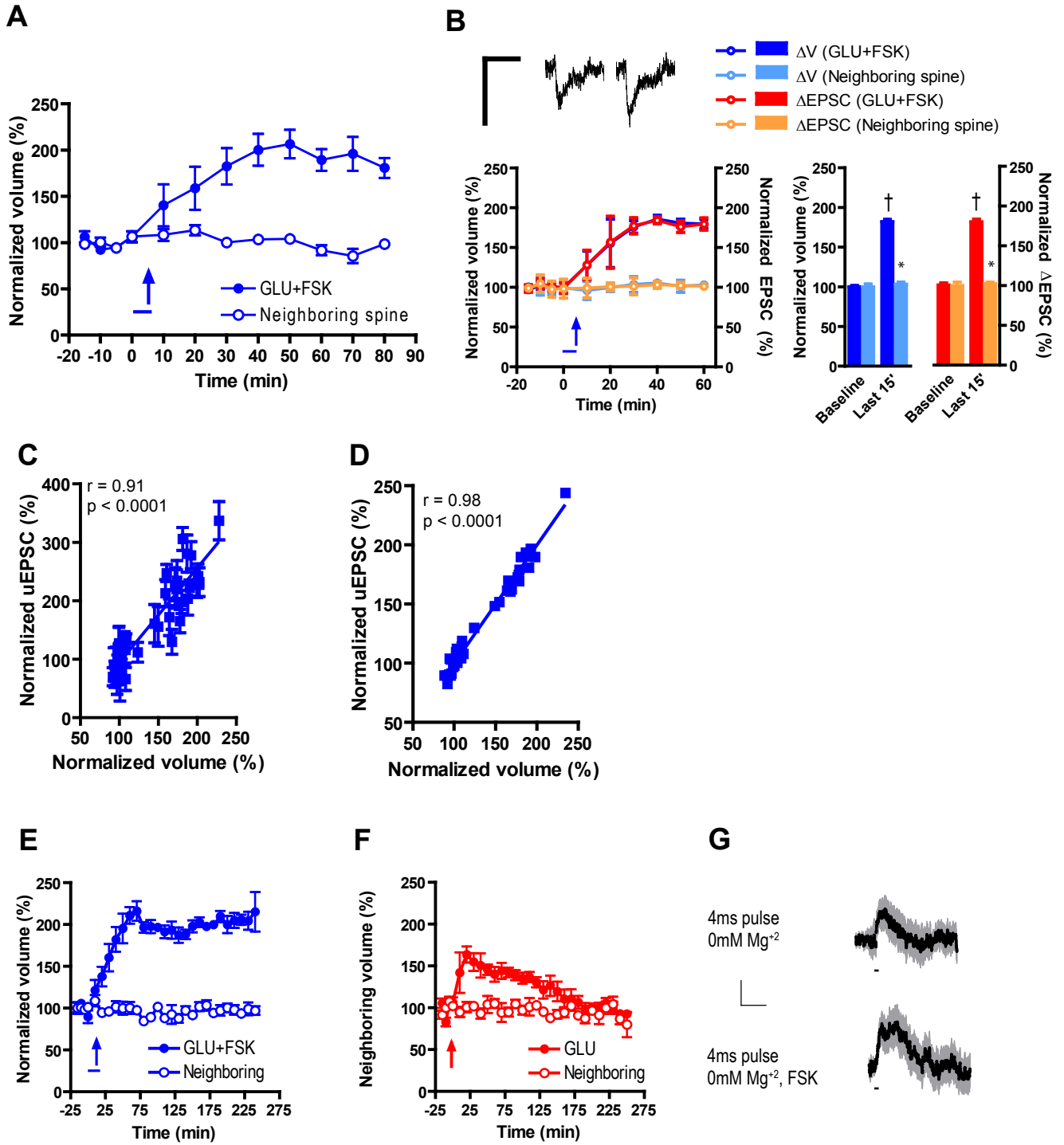


Figure S2

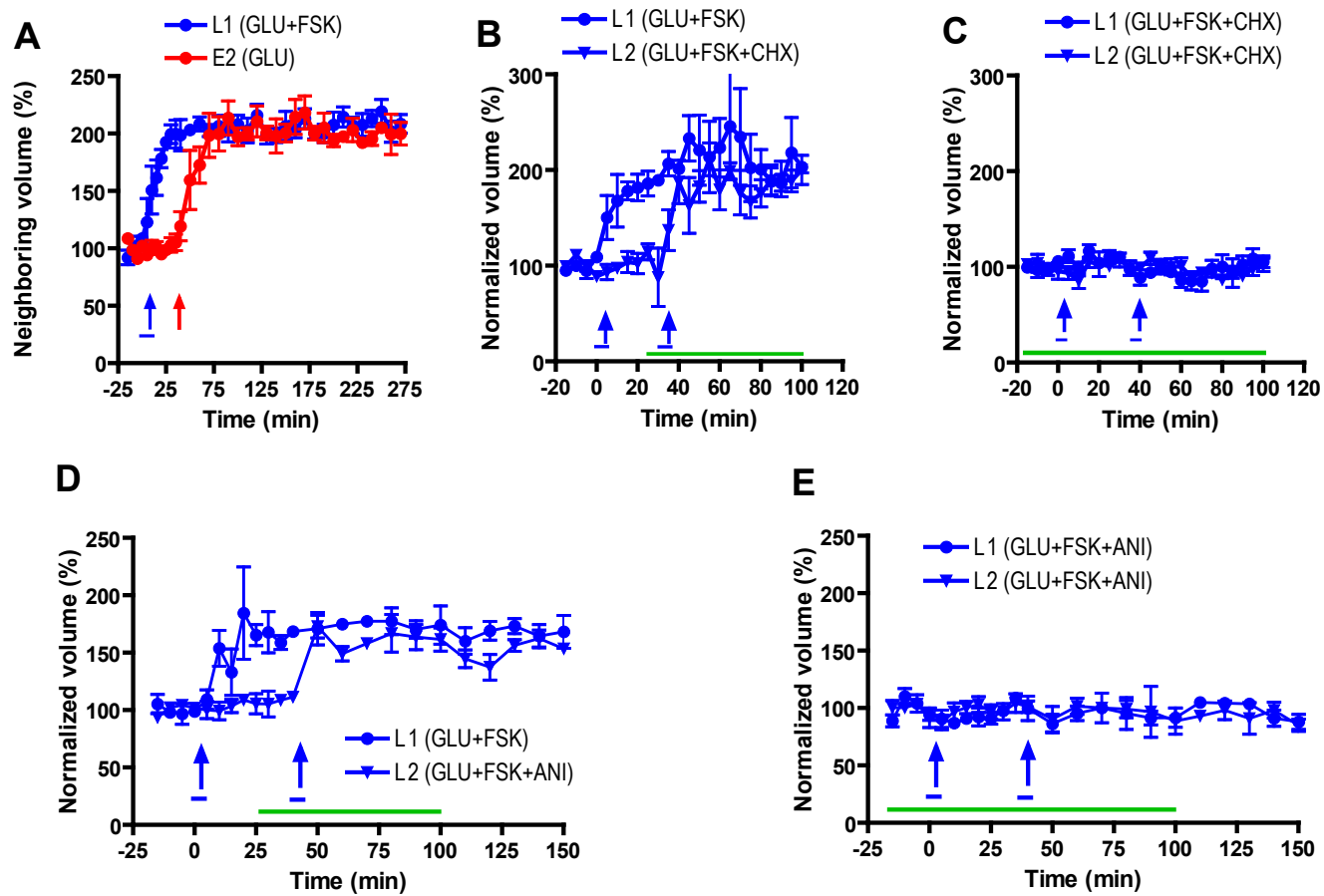


Figure S3

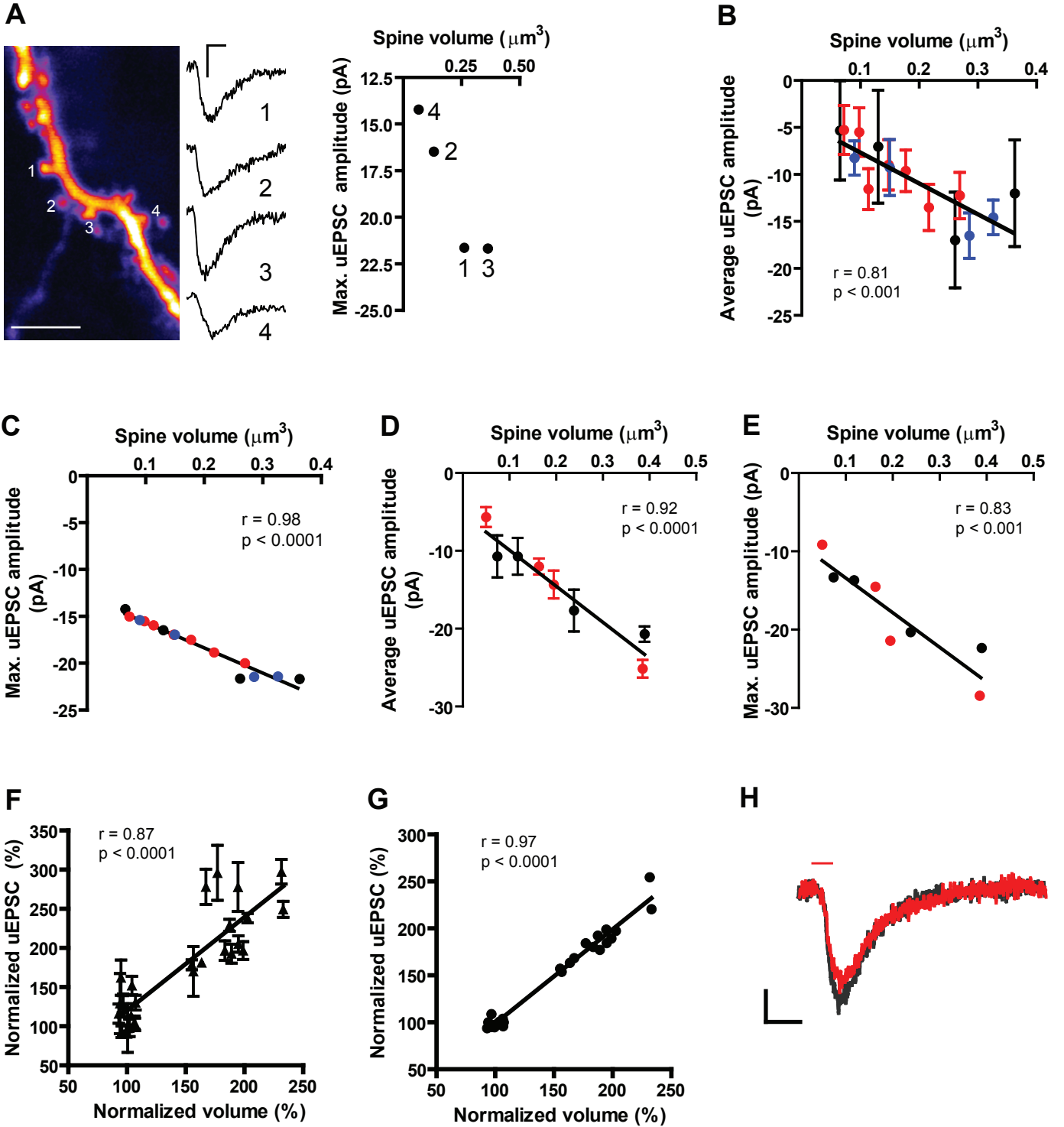


Figure S4

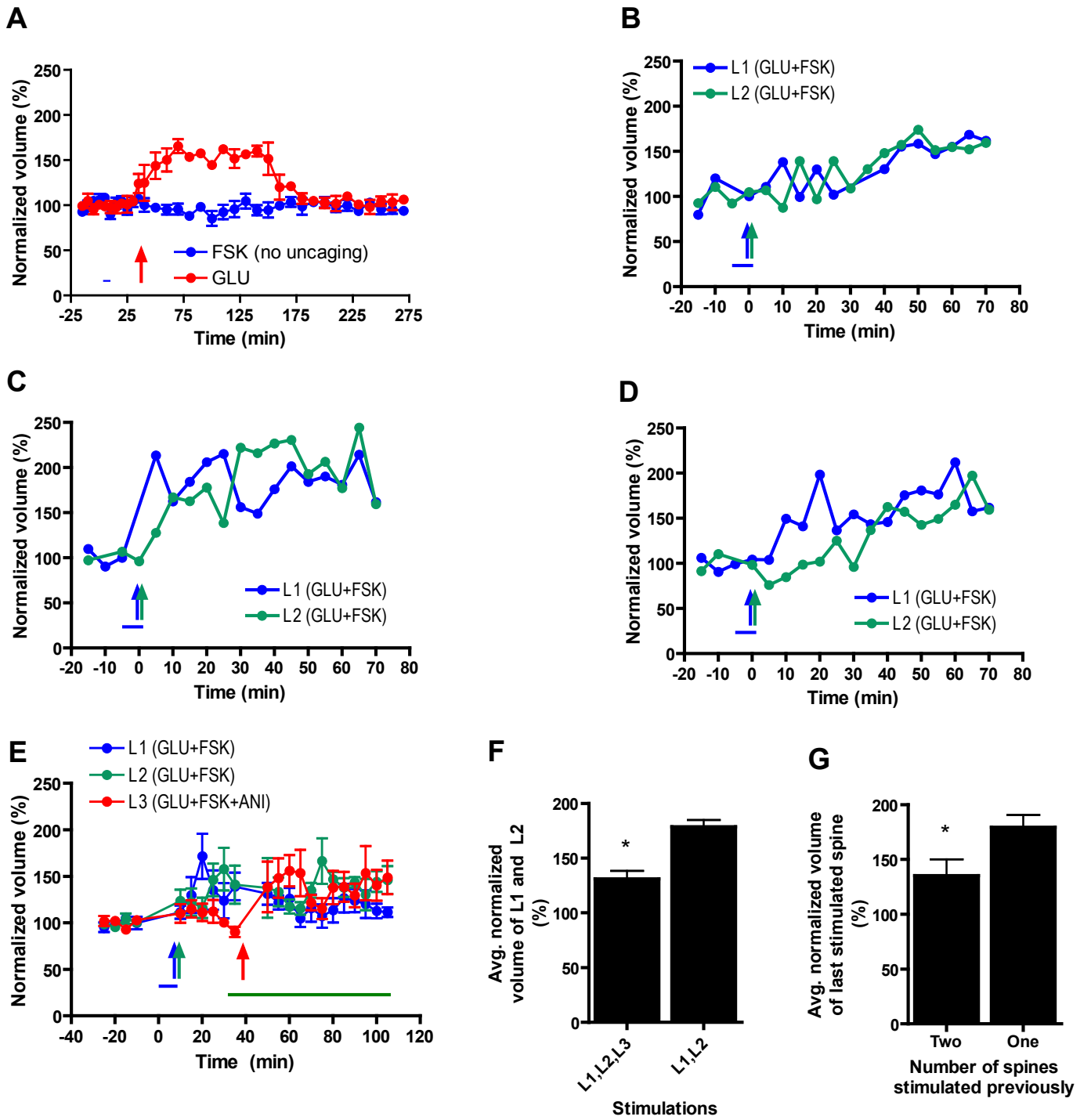


Figure S5

